

Analytical Methods

Accepted Manuscript



This is an *Accepted Manuscript*, which has been through the Royal Society of Chemistry peer review process and has been accepted for publication.

Accepted Manuscripts are published online shortly after acceptance, before technical editing, formatting and proof reading. Using this free service, authors can make their results available to the community, in citable form, before we publish the edited article. We will replace this *Accepted Manuscript* with the edited and formatted *Advance Article* as soon as it is available.

You can find more information about *Accepted Manuscripts* in the [Information for Authors](#).

Please note that technical editing may introduce minor changes to the text and/or graphics, which may alter content. The journal's standard [Terms & Conditions](#) and the [Ethical guidelines](#) still apply. In no event shall the Royal Society of Chemistry be held responsible for any errors or omissions in this *Accepted Manuscript* or any consequences arising from the use of any information it contains.

CeO₂-MWCNT nanocomposite based electrochemical sensor for acetaldehyde

Rayammarakkar M. Shereema^{a,b}, Sindhu R. Nambiar^a, S. Sharath Shankar^{a*} and Talasila P. Rao^{a,b*}

^a*Chemical Sciences & Technology Division (CSTD),*

CSIR-National Institute for Interdisciplinary Science & Technology (CSIR-NIIST),

*Trivandrum 695019, INDIA. *e-mail: tprasadarao@rediffmail.com*

^b*Academy of Scientific and Innovative Research (AcSIR), New Delhi 110001, India.*

Abstract

The present study endeavours to build a new, highly sensitive and selective electrochemical sensor with CeO₂-MWCNT nanocomposite film, which enhances the sensing platform to detect acetaldehyde. The chemically synthesised CeO₂ nanoparticles were subjected to adsorb on MWCNT. Thus prepared nanocomposite was characterized by XRD, SEM and Impedance spectroscopy. Drop to drop method was employed in the preparation of CeO₂-MWCNT modified glassy carbon electrode which could sense nanomolar levels of acetaldehyde by cyclic voltammetry. Under optimal conditions, the developed sensor detected acetaldehyde in the concentration range of 10⁻⁸ to 10⁻⁵ M with a detection limit of 7.4×10⁻⁹ M accompanied with a good precision of 1.6 % at 10⁻⁶ M of acetaldehyde. Moreover, it exhibited reasonably good selectivity towards acetaldehyde in conjunction with different co-existing organic species and was successfully applied to synthetic fruit juice samples.

Key words: Multiwalled carbon nanotubes-CeO₂ nanocomposite film, Acetaldehyde, Synthetic fruit juices.

1 INTRODUCTION

The incomplete combustion of petroleum fuels and biomass produces aldehydes which are ubiquitous air pollutants¹. Inhalation of acetaldehyde may result in bronchitis, dotiness, protein denaturation and sometimes even death²⁻⁴. Acetaldehyde is found in many food items including, ripe fruits, beverages, vegetables, cheese and other dairy products. Ripened fruit contains about 80% of acetaldehyde than unripe ones. In beverages, it is formed due to the enzymatic oxidation of alcohol. Therefore, the main pathways by which acetaldehyde enter our body includes air, water, alcohol drinking and tobacco smoke. The increased concentration of acetaldehyde in our body favours its reaction with DNA due to its strong electrophilic property which could induce mutagenesis and carcinogenesis⁵⁻⁶. Being toxic at low concentration and carcinogenic when exposed for prolonged time, aldehyde detection is significantly important for monitoring environmental and domestic pollution⁷⁻⁹, as well as food sophistication or contamination from packaging. Hence, the development of sensitive, rapid, simple, and low-cost devices for acetaldehyde detection is urgent and important.

There are limited reports available on acetaldehyde detection. Abbas et al. employed neutral red- sulfite-acetaldehyde system to detect traces of acetaldehyde by developing a kinetic method¹⁰. Yashuhara and shibamoto detected it using gas chromatography with a nitrogen-phosphorus detector¹¹. A gas chromatographic method using electron capture detector was adopted for the determination of the same by Mori et al.¹². High performance liquid chromatography has been used for the same purpose¹³⁻¹⁶. Determination of aliphatic aldehydes in aqueous solution by the inhibition of luminol chemiluminescence induced by hydrogen peroxide in the presence of potassium hexacyanoferrate has been reported¹⁷. Since all these methods converted acetaldehyde to some other form to detect it, they are considered to be

1
2
3 indirect methods. However, there were studies reported to have detected acetaldehyde as it is by
4
5 amperometry-based sensor¹⁸.
6
7

8 Cerium oxides mark their distinctive application as excellent catalysts. Over the years,
9
10 cerium oxide and cerium oxide-based materials have been investigated as structural and
11
12 electronic promoters of heterogeneous catalytic reactions. One of the most familiar applications
13
14 in this field is the utilization of CeO₂ as the key component in three-way catalysts for the
15
16 treatment of exhaust gas from automobiles¹⁹. Among different lanthanide oxides, ceric oxides
17
18 are widely used due to their excellent catalytic properties²⁰⁻²². CeO₂ and its nanocomposite films
19
20 like CeO₂-BaTiO₃, cerium oxide (NanoCeO₂)-chitosan were also explored for applications in
21
22 electronic devices²³ and biosensors^{24, 25}. Composite materials based on CNTs and metal oxide
23
24 nanomaterials integrate their unique characters and functions and may also exhibit some new
25
26 properties caused by the cooperative effects between the two kinds of materials²⁶⁻³⁰. Therefore,
27
28 these composite materials have shown very attractive potential applications in many fields.
29
30
31
32
33

34 In this article we describe a direct method for the determination of acetaldehyde with
35
36 CeO₂-MWCNT/GCE by cyclic voltammetry. We mainly concentrated on CeO₂-MWCNT
37
38 nanocomposite based on the report that, CeO₂ converts acetaldehyde into acetic acid by donating
39
40 its labile oxygen atom present in their crystal lattices due to its fluorite structure. Here, Ce⁴⁺ is
41
42 reduces itself into Ce³⁺ by oxidizing molecules on its surface³¹.
43
44
45

46 **2 Experimental**

47 **2.1 Chemicals and reagents**

48
49 Acetaldehyde, multi walled carbon nanotube and cerium oxide was purchased from
50
51 Aldrich, Milwaukee, WI, USA. Deionised double distilled water was used in the preparation of
52
53 working solutions. All other chemicals were of analytical reagent grade (E Merck, Mumbai,
54
55 India) and were used as received, without any further purification. Potassium nitrate solution of
56
57
58
59
60

1
2
3 pH 6 was used as the supporting electrolyte in all the electrochemical experiments. Stock
4
5 solution of 0.1 M acetaldehyde was freshly prepared for each series of experiments.
6
7

8 **2.2 Instrumentation**

9
10 Electrochemical measurements were done using a three-electrode cell, with a glassy
11 carbon electrode (3 mm in diameter) as working electrode, Pt wire as auxiliary electrode and
12 Ag/AgCl electrode as reference electrode using a VSP-potentiostat/galvanostat (Biologic Science
13 Instruments). The Oakton pH 700 meter, Germany, was used to measure pH. The size and
14 morphology were examined with the aid of a scanning electron microscope (SEM), JEOL,
15 Model JSM 5600 LV, Tokyo, Japan. UV- Visible spectra were recorded with a computer
16 controlled double beam UV-Vis spectrophotometer UV-2401PC (Shimadzu, Kyoto, Japan), X-
17 ray diffraction (XRD) pattern of the samples were recorded on a Philips X'pert diffractometer
18 (XRD, X'Pert Pro MPD) with CuK α radiation (1.5406Å).
19
20
21
22
23
24
25
26
27
28
29
30
31

32 **2.3 Preparation of CeO₂-MWCNT nanocomposite and fabrication of CeO₂-MWCNT/GC electrode**

33
34 CeO₂ nanoparticles were synthesized by chemical method reported in the literature³². An
35 appropriate amount of MWCNT (0.25 %) was added to the synthesized CeO₂ and sonicated for
36 30 minutes to form a homogeneous solution. The Van der Waals force of attraction between
37 CeO₂ and MWCNT made CeO₂ to easily attach to the walls of MWCNT. This benefit was used
38 for the fabrication of CeO₂-MWCNT/GC modified electrode. The GC electrode was polished
39 with alumina slurry followed by sonication. On to this fine surface of GC, 5 μ L of the above
40 suspension was added by drop to drop and air dried to obtain the CeO₂-MWCNT/GC modified
41 electrode. Thus developed modified electrode was used to detect acetaldehyde in 0.1M KNO₃ of
42
43
44
45
46
47
48
49
50
51
52
53
54
55
56
57
58
59
60
pH 6.

2.4 Electrochemical measurements

A freshly prepared solution of acetaldehyde ($1\mu\text{M}$) was added to an electrochemical cell containing 10 ml of 0.1M KNO_3 as supporting electrolyte (pH 6). Cyclic voltammetric curves were plotted by scanning the potential from -0.4 to 1.2 V at a scan rate of 50 mV s^{-1} . The acetaldehyde quantification was achieved by measuring the oxidation peak current at 0.78V.

3 Results and Discussions

3.1 Characterization studies

The prepared CeO_2 -MWCNT nanocomposite was characterized by the following methods.

3.1.1 Spectral and morphological characterization

Fig.1 showed the XRD pattern of CeO_2 and CeO_2 -MWCNT nanocomposite in the range of 10 - 70° . The four angles at 28.5° , 33.1° , 47.5° and 56.3° correspond to (111), (200), (220) and (311) planes of the face centered cubic phase of CeO_2 (JCPDS 78-0694). After incorporating MWCNT two additional peaks were observed at 26.2° and 42.1° corresponding to the plane (002) and (101) which is the clear evidence of adsorption of CeO_2 on MWCNT. From Scherrer formula,

$$D = K\lambda/\beta \cos\theta$$

Where D is the crystallite size, K is the Sherrer constant (0.89), λ is the wave length of Cu $\text{K}\alpha$ radiation (0.15406 nm), β is FWHM (full width of peak intensity at half maximum) in

1
2
3
4
5
6
7
8
9
10
11
12
13
14
15
16
17
18
19
20
21
22
23
24
25
26
27
28
29
30
31
32
33
34
35
36
37
38
39
40
41
42
43
44
45
46
47
48
49
50
51
52
53
54
55
56
57
58
59
60

radians, θ is the peak (1 1 1) position in degrees, particle size of CeO₂ was calculated and was found to be 15-25 nm.

Fig.2 (a), (b), and (c) showed the scanning electron micrographs of CeO₂, MWCNT and CeO₂-MWCNT nanocomposites. It was observed that CeO₂ possessed the spherical shape with size 10-30 nm (a) and MWCNT the tubular form (b). The spherically shaped CeO₂ stucked on the surface of MWCNT and it is the concrete indication of the CeO₂-MWCNT nanocomposite.

3.1.2 UV-Visible absorption spectrum

Fig. 3 showed the UV-Visible absorption spectrum of CeO₂ and CeO₂-MWCNT nanocomposite. A well-defined sharp and strong absorbance peak at 300 nm was observed which is due to the Ce⁴⁺, indicating a narrow and uniform particle size distribution obtained via this route. There was no change in CeO₂ absorbance after the addition of MWCNT, which suggests that MWCNT has no influence on the size and structure of the CeO₂ nanoparticles. Hence, the role of MWCNT was to provide a better surface for the oxidation of acetaldehyde, thereby increasing the current, which was confirmed from electrochemical characterization studies.

3.2 Electrochemical characterization

3.2.1 Electrochemical Impedance Spectroscopy

EIS is a commonly used characterization technique for studying the impedance changes of the electrode surface during modification process. In Nyquist plot, the semi-circular or real portion is related to electron transfer resistance R_{ct} and linear or imaginary part is related to controlled diffusion process. Electron transfer Resistance is dependent on the diameter of the semi-circular portion. Large semicircle with high R_{ct} means (contributes) the system has higher resistance to the flow of electrons. Fig.4 shows EIS of bare GCE (a), CeO₂/GCE (b) and CeO₂-

1
2
3 MWCNT/GCE (c) in $\text{Fe}(\text{CN})_6^{3-/4-}$ system. Inset is the equivalent circuit used to analyse the
4
5 impedance behavior. The small semicircular portion of GCE implies it has low resistance
6
7 towards the electron transfer process. After modifying with CeO_2 , the diameter of semicircle was
8
9 increased with R_{ct} value 489Ω , indicating the CeO_2 nanoparticles hindered the electron transfer
10
11 of the electrochemical probe of $\text{Fe}(\text{CN})_6^{3/4-}$ and this hindrance was decreased ($R_{\text{ct}} = 401\Omega$) after
12
13 incorporating MWCNT with CeO_2 nanoparticles. These results showed the efficiency of CeO_2 -
14
15 MWCNT/GCE.
16
17
18
19
20

21 3.2.2 Cyclic Voltammetric analysis

22
23 In comparison to the bare GC and CeO_2/GC electrodes, the CeO_2 -MWCNT/GC electrode
24
25 provided more electroactive surface for the oxidation of acetaldehyde. This was confirmed
26
27 through the cyclic voltammeteric experiments of different electrodes in 1mM $\text{K}_3[\text{Fe}(\text{CN})_6]$
28
29 solution. Fig.5 represented the cyclic voltammograms of bare GC (curve a), CeO_2/GC (curve b)
30
31 and CeO_2 -MWCNT/GC (curve c) electrode in 1 mM $\text{K}_3[\text{Fe}(\text{CN})_6]$ with 0.1 M KCl as the
32
33 supporting electrolyte. At bare GC, ferricyanide showed anodic peak at 170 mV with peak
34
35 current $11\mu\text{A}$ and cathodic peak at 98 mV with $13\mu\text{A}$. ΔE_p for bare GC was found to be 72
36
37 mV, which was an indication of quasi reversible nature of bare GC. In CeO_2/GCE , the anodic
38
39 peak potential shifted to more positive side i.e., 196 mV and cathodic peak current potential
40
41 shifted to more negative side i.e., 93 mV with ΔE_p 103 mV. Sensitivity of $\text{K}_3[\text{Fe}(\text{CN})_6]$
42
43 increased remarkably, which could be explained by the change of particle size and increase in
44
45 electroactive surface area at CeO_2/GCE , but at the same time process still remained quasi
46
47 reversible. After adding MWCNT to CeO_2/GCE , a rapid and a sharp increase of the both anodic
48
49 ($28\mu\text{A}$) and cathodic current ($29\mu\text{A}$) was observed with shift in both anodic (202 mV) and
50
51 cathodic peak (123 mV) potentials. ΔE_p at CeO_2 -MWCNT/GCE was 60 mV, which implied the
52
53
54
55
56
57
58
59
60

1
2
3 electrochemical process had changed to reversible indicating the good performance of the
4 modified electrode. Therefore, the electrocatalytic effect is higher in CeO₂-MWCNT/GC
5 electrode as compared to CeO₂/GC and bare GC electrodes.
6
7
8
9

10 Fig.6 showed the cyclic voltammograms of acetaldehyde in a potential range of -0.4 to
11 1.2 V at a scan rate of 50 mV/s in 0.1M KNO₃ solution at bare GC (curve a), MWCNT/GC
12 (curve b) CeO₂/GC (curve c) and CeO₂-MWCNT/GC (curve d) electrodes. There were no peaks
13 observed at bare GC, MWCNT/GC electrodes. One broad anodic peak at 0.88 V due to the
14 oxidation of Ce was generated at the CeO₂/GC electrode, which further sharpened and shifted to
15 0.8 V with an increase in current at the CeO₂-MWCNT/GCE. The broadened reduction peak
16 appeared at 300 mV on CeO₂/GC was shifted to 400 mV on CeO₂-MWCNT/GCE representing
17 the quasi reversible nature of both CeO₂/GCE and CeO₂-MWCNT/GCE.
18
19
20
21
22
23
24
25
26
27
28
29

30 3.3 Voltammetric analysis of acetaldehyde at CeO₂-MWCNT/GCE

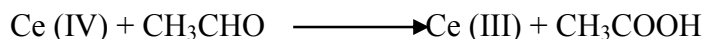
31 Fig.7 (a) showed the cyclic voltammetric curves of acetaldehyde with different
32 concentrations in 0.1 M KNO₃ buffer of pH 6.0. For each addition of acetaldehyde there was a
33 decrease in peak current. When the acetaldehyde concentration increased, more CeO₂ would be
34 used for the conversion of acetaldehyde to acetic acid, this could be the reason for decline in the
35 peak current. The plot of peak current vs. [acetaldehyde] (Fig.7(b(i))) gives dual linearity, one at
36 lower concentration range from 0.01 to 0.5 μM and other in higher concentration range from 0.5
37 to 10 μM. Which means the fabricated electrode could be applied for a wide range of
38 concentrations. For the calculation of limit of detection, a plot of peak current vs. log
39 [acetaldehyde] was drawn. Again, a good linear graph with a wider range of concentrations, 10⁻⁸
40 to 10⁻⁵M was obtained (Fig.7(b(ii))). The limit of detection was calculated as 7.4x10⁻⁹M based on
41 3 times the standard deviation of the blank value. The relative standard deviation was found to be
42
43
44
45
46
47
48
49
50
51
52
53
54
55
56
57
58
59
60

1
2
3 1.6% for 10 replicate determinations of 10^{-6} M of acetaldehyde, which revealed the extremely
4 high precision of designed acetaldehyde sensor. Moreover, the developed CeO_2 -MWCNT/GCE
5 was able to produce same current for a period of one week; this showed the stability of the
6 electrode.
7
8
9
10

11 12 **3.4 Mechanism**

13
14
15 Possible mechanism for this electrode process could be explained as follows, Ce^{4+} is
16 reduced itself into Ce^{3+} by oxidizing the molecules on its surface. The energy between 4f and 5d
17 is almost same so we can easily switch off $\text{Ce}^{4+}/\text{Ce}^{3+}$ inter conversion by applying low potential
18 energy. In fluorite structure of CeO_2 , the oxygen atom can easily move around the crystal
19 allowing the cerium to reduce or oxidize the molecule on its surface. Hence the CeO_2 can easily
20 convert acetaldehyde into acetic acid by donating its labile oxygen atoms to the acetaldehyde.
21
22
23
24
25
26
27
28

29 Scheme 1 gave the schematic representation of this mechanism.
30



36 **3.5 Effect of scan rate**

37
38 The effect of scan rate on the electrocatalytic behavior of the modified electrode towards
39 the oxidation of acetaldehyde was studied by cyclic voltammetry. Fig.S1 (a) & Fig.S2(a) show
40 the cyclic voltammograms of oxidation of acetaldehyde at various scan rates (20 to 90 mVs^{-1}) at
41 the CeO_2 -MWCNT/GC modified electrode and CeO_2 /GC electrode respectively. It could be
42 perceived from the above CV's that with an increase in scan rate, the peak potential for the
43 electro-oxidation of acetaldehyde shifts to more positive potentials, suggesting a kinetic
44 limitation in the reaction between the redox sites of modified electrode and acetaldehyde. In
45 addition, catalytic current increases with increasing scan rate, because in short scale experiments
46 there is no enough time for catalytic reaction to take place completely.
47
48
49
50
51
52
53
54
55
56
57
58
59
60

In order to obtain information about the rate determining step, the Tafel slope was drawn using the following equation, for a diffusion controlled process,

$$E_p = (b/2) \log v + \text{constant}$$

Based on the above equation, from the Tafel plot (Fig. S1 (b)) the slope of E_p vs. $\log v$ is $b/2$ where b indicates the Tafel slope. The slope of E_p vs. $\log v$ for CeO_2 -MWCNT/GC electrode was found to be 0.0809. This slope indicates an electron transfer co-efficient of $\alpha = 0.73$ for a one electron transfer process, which is the rate determining step. Similarly for CeO_2 /GC modified electrode, α value was 0.59 (Fig. S2 (b)). On the basis of the slopes of the linear dependence of the anodic peak currents on the square root of the potential sweep rates (Fig. S1 (c), fig.S2(c)), by Randle-Sevcik equation

$$I_p = (2.99 \times 10^5) \alpha^{0.5} n^{1.5} A C D^{0.5} v^{0.5}$$

where I_p is the peak current, A is the electrode surface area, D is the diffusion co-efficient and C is the bulk concentration, the diffusion coefficient of acetaldehyde was calculated to be $5.46 \times 10^{-3} \text{ cm}^2/\text{s}$ and $1.55 \times 10^{-2} \text{ cm}^2/\text{s}$ for CeO_2 /GC and CeO_2 -MWCNT/GC modified electrode respectively.

The reaction (adsorption controlled or diffusion controlled) that controlled acetaldehyde oxidation on CeO_2 /GC and CeO_2 -MWCNT/GC was studied from the plots of I_p Vs ϑ (Fig.S1 and S2 (d)) and I_p Vs $\vartheta^{0.5}$. In case of CeO_2 /GC electrode, I_p Vs ϑ is more linear than I_p Vs $\vartheta^{0.5}$ indicating adsorption controlled processes. But in CeO_2 -MWCNT/GC the greater linearity of the I_p vs. $v^{0.5}$ plot indicates the mass transfer being predominately diffusion controlled.

3.6 Optimization studies for the determination of acetaldehyde at the CeO₂-MWCNT/GC modified electrode

In order to attain maximum sensitivity, the effect of concentration of CeO₂ and weight percentage of MWCNT was studied by varying the volume of CeO₂ and the weight percentage of MWCNT in the nanocomposite. While keeping the weight percentage of MWCNT constant, volume of CeO₂ suspension was varied from 250-1000 μ l. As it can be seen from, fig.S3, 500 μ L gave maximum current, further increment in concentration of CeO₂ from 500 μ L the peak current decreased and the anodic peak became broad just like the peak obtained in CeO₂ alone, still it senses acetaldehyde from 10⁻⁸ M. By maintaining the concentration of CeO₂ at 500 μ L we varied the weight percentage of MWCNT from 0.15 to 0.90 % and observed a maximum sensitivity at 0.25 %, fig.S4. Further increase in weight percentage of MWCNT, decreased the sensitivity with increase in current, this could be due to the fact that the MWCNT provided its surface area for the adsorption of CeO₂ and also considerably contributed to the electron transfer process. Hence 500 μ L of CeO₂ with 0.25% MWCNT was considered to be optimum conditions for further analysis.

Likewise, the effect of drop to drop volume of the nanocomposite on the GC was optimized and 5 μ L exhibited better sensitivity. While increasing the drop to drop volume above 5 μ L the sensitivity shrunk, this could be attributed to the increasing film thickness and the possibility of peeling off from the electrode surface (Fig.S5).

3.7 Effect of electrolyte and pH

The different parameters which may possibly affect the electrochemical determination of acetaldehyde were also studied. Effect of different supporting medium including, sodium chloride, potassium chloride, sodium acetate, potassium nitrate, ammonium acetate and sodium

1
2
3 di-hydrogen phosphate electrolyte towards the electrochemical determination of acetaldehyde on
4 the surface of CeO₂-MWCNT/GC electrode was analysed. Among which potassium nitrate gave
5 better response for acetaldehyde sensing and was used as the supporting electrolyte for further
6 analysis.
7
8
9
10

11
12 The effect of the pH of the supporting electrolyte on the electrochemical behaviour of the
13 sensor was investigated over the range of 4.0–9.0. The response current and sensitivity of the
14 sensor increased with increasing pH values from 4.0 to 6.0 and then decreased with further
15 increase in pH (Fig. S6). This could be due to the fact that CeO₂ would act as a strong oxidising
16 agent when they are in the acidic medium.
17
18
19
20
21
22
23

24 **3.8 Comparison with reported acetaldehyde sensors**

25
26 Table 1 depicts the comparative studies of the current method with the reported
27 acetaldehyde sensing methods. In comparison with hitherto reported methods, the current
28 method had wider calibration range and lower detection value. The only sensor which comes
29 closest to the developed sensor is Au-nafion sensor with limit of detection 23nM but it offers
30 only a small calibration range 0.025- 0.5 μM.
31
32
33
34
35
36
37
38

39 **3.9 Selectivity studies and analysis of synthetic mixtures of fruit juice**

40
41 Since acetaldehyde is present in most of the fruits, the selectivity of the CeO₂-
42 MWCNT/GC modified electrode for acetaldehyde sensing was investigated under optimised
43 conditions by testing the response to several compounds that are usually present in fruit juice.
44 Among the different interferents, ethanol interferes even in equal amount but glucose, fructose,
45 and glycerol do not interfere up to 100 folds. Cations like K⁺ and Na⁺ are not interfering in the
46 acetaldehyde oxidation.
47
48
49
50
51
52
53
54

55 Fig.8 showed the peak current of 10⁻⁶ M of acetaldehyde and other interferents, which
56 indicated that the developed electrode showed good selectivity towards acetaldehyde from the
57
58
59
60

1
2
3 potential interfering species and could be applied to determine its concentration in the fruit juice
4 samples. Therefore, the developed modified electrode was applied for the determination of
5 acetaldehyde in synthetic mixture of fruit juice using the standard addition method and the
6 recoveries of acetaldehyde are presented in Table 2.
7
8
9
10
11
12
13

14 **4 Conclusions**

15
16 A voltammetric sensor based on CeO₂-MWCNT nanocomposite was designed for
17 acetaldehyde sensing. MWCNT can improve the stability of the modified electrode, reduce the
18 agglomeration level of CeO₂ nanoparticles, and increase the electron transfer rate. The catalytic
19 oxidation of acetaldehyde was found to be highly sensitive at the nano-CeO₂-MWCNT/GC
20 because of the synergistic effect of nano-CeO₂ and MWCNT. A lower detection limit of 7.4×10
21 $^{-9}$ mol/L, wide linear range from 10^{-8} to 10^{-5} mol/L, excellent selectivity, good stability and
22 repeatability gives it the potential application in acetaldehyde sensing. Also interference study
23 showed reasonably good selectivity and hence the developed modified electrode is suitable for
24 measurement of acetaldehyde in fruit juice samples.
25
26
27
28
29
30
31
32
33
34
35
36
37
38
39

40 **Acknowledgements**

41
42 The authors are thankful to Dr. K. V. Radhakrishanan for his fruitful discussions
43 during various stages of the work. Ms. Shereema and Ms. Sindhu R. Nambiar acknowledge
44 CSIR, New Delhi, India for the award of Senior Research Fellowships. The authors are thankful
45 to CSIR, New Delhi, India for providing funds through the MULTIFUN project (CSC0101). The
46 authors thank Mrs. Lucy Paul for SEM analysis.
47
48
49
50
51
52
53
54

55 **References**

56
57
58
59
60

1. G. D. Silva, and J. W. Bozzelli, *J. Phys. Chem. A*, 2006, **110**, 13058–13067.
2. P. J. O'Brien, A. G. Siraki and N. Shangari, *Crit. Rev. Toxicol.*, 2005, **35**, 609–662.
3. S. Stein, Y. B. Lao, I. Y. Yang, S. S. Hecht, and M. Moriya, *Mutation Research*, 2006, **608**, 1–7.
4. L. Chen, M. Y. Wang, P. W. Villalta, X. H. Luo, R. Feuer, J. Jensen, D. K. Hatsukami, and S. S. Hecht, *Chem. Res. Toxicol.*, 2007, **20**, 108–113.
5. M. Uebelacker and D. Lachenmeier, *Journal of Automated Methods and Management in Chemistry* 2011, **12**, 13-16.
6. Y. Qiao, B. J. Xie, Y. Zhang, Y. Zhang, G. Fan, X. L. Yao and S. Y. Pan, *Molecules*, 2008, **13**, 1333-1344.
7. H. Nanto, Y. Yokoi, T. Mukai, J. Fujioka, E. Kusano, A. Kinbara, and Y. Douguchi, *Mater. Sci. Eng. C*, 2000, **12**, 43-48.
8. H. Fromme, D. Heitmann, S. Dietrich, R. Schierl, W. Korner, M. Kiranoglu, A. Zapf, and D. Twardella, *Gesundheitswesen*, 2008, **70**, 88-97.
9. A. Roche, V. Jacob, C. Garcia, P. Baussand, and P. Foster, *Sensors and Actuators B: Chemical*, 1999, **59**, 103-107.
10. A. Afkhami, H. Parham, and M. Rezaei, *Anal. Lett.*, 2000, **33**, 527–538.
11. A. Yasuhara, and T. Shibamoto, *J. Chromatogr. A*, 1994, **672**, 261–266.
12. Y. Mori, K. Tsuji, S. Setsuda, S. Goto, S. Onodera, and H. Matsushita, *J. Tox. Env. Health*, 1996, **42**, 500–506
13. S. Helmut, *Gefahrstoffe - Reinhaltung der Luft*, 1997, **57**, 75–78.
14. F. Lipari, and S. J. Swarin, *J. Chromatogr.*, 1982, **247**, 297–306.
15. M. S. Gandelman, and J. W. Birks, *J. Chromatogr.*, 1982, **242**, 21–31.
16. TO-O5, USEPA, Chemical/name index to EPA test methods 600 4-89-017 (2001).

- 1
2
3 17. B. Vogin, F. Baronnet, and J. C. Andre, *Anal. Chim. Acta*, 1982, **142**, 293–297.
4
5
6 18. P. Jacquinet, A.W. E. Hodgson, B. Muller, B. Wehrli, and P. C. Hauser,
7
8 *Analyst*, 1999, **124**, 871–876.
9
10 19. A. Trovarelli, *Catal. Rev-Sci. Eng.*, 1996, **38**, 439-520.
11
12 20. H.C. Yao, and Y. F. Y. Yao, *J. Catal.*, 1984, **86**, 254-265
13
14 21. M. Haneda, T. Mizushima, and N. Kakuta, *J. Chem. Soc. Faraday Trans.*, 1995, **91**, 4459-
15
16 4465.
17
18 22. K. Fukui, Y. Namai, and Y. Iwasawa, *Appl. Surf. Sci.*, 2002, **188**, 252-256.
19
20 23. S. M. Kim, and S.Y. Lee, *Physica C*, 2001, **351**, 42-44.
21
22 24. B. D. Malhotra and A. Kaushik, *Thin Solid Films*, 2009, **518**, 614-620
23
24 25. S. Saha, S. K. Arya, S. P. Singh, K. Sreenivas, B. D. Malhotra, and V. Gupta, *Biosensors*
25
26 *and Bioelectronics*, 2009, **24**, 2040-2045.
27
28 26. G. G. Wildgoose, C. E. Banks and R. G. Compton, 2006, *Small*, **2**, 182-193.
29
30 27. V. Georgakilas, D. Gournis, V. Tzitzios, L. Pasquato, D.M. Guldi, and M. Prato,
31
32 *J. Mater. Chem.*, 2007, **17**, 2679-2694.
33
34 28. X. G. Hu and S. J. Dong. *J. Mater. Chem.*, 2008, **18**,1279-1295.
35
36 29. D. Vairavapandian, P. Vichchulada, and M. D. Lay, *Anal. Chim. Acta.*, 2008, **626**, 119-129.
37
38 30. X. Peng, J. Chen, J. A. Misewich, and S. S.Wong, *Chem. Soc. Rev.*, 2009, **38**, 1076-1098.
39
40 31. H. Idriss, *Platinum Metals Rev.*, 2004, **48**, 105-115.
41
42 32. W. Yan, W. Guangfeng, L. Maoguo, W. Cong, and F. Bin, *Microchim Acta*, 2007, **158**, 269–
43
44 274.
45
46 33. A. A sacks, L. L okumura, M. F. D. Oliveira, M. V. B.zanoni, and N. R. stradiotto,
47
48 *Analytical Sciences*, 2005, **21**, 441-444.
49
50
51
52
53
54
55
56
57
58
59
60

- 1
2
3
4
5
6
7
8
9
10
11
12
13
14
15
16
17
18
19
20
21
22
23
24
25
26
27
28
29
30
31
32
33
34
35
36
37
38
39
40
41
42
43
44
45
46
47
48
49
50
51
52
53
54
55
56
57
58
59
60
34. T. Noguier, and J. L Marty, *Anal. Lett.* 1997, 30, 1069-1080
35. M. E. Ghica, R. Pauliukaite , N. Marchand , E. Devic , and C. M. A. Brett , *Analytica Chimica Acta*, 2007, **591**, 80–86.
36. G. Karim-Nezhad, P. S. Dorraji, and B. Z. Dizajdizi, *Anal. Bioanal. Electrochem.*, 2011, **3**, 1-13.
37. T. Noguier, and J. L. Marty, *Enzyme and Microbial Technology*, 1995, **17**, 453–456.

TABLES

Table 1. Comparison with reported acetaldehyde sensing methods

| Method | Modification | Linear calibration Range | Detection limit(nM) | Reference |
|-----------------------|--------------------------------------------------------------------------------------------------------------|---------------------------|---------------------|--------------|
| HPLC-electrochemistry | GC | 68 to 6800 μ M | 86 | [33] |
| Amperometry | Au-nafion | 0.025 to 0.50 μ M | 23 | [18] |
| Amperometry | AIDH, NADH oxidase and NADs in a polyvinyl alcohol bearing styryl pyridiruum groups (PVA-SbQ) matrix/Pt disk | 0.5 to 330 μ M | - | [34] |
| Amperometry | PNR/sol-gel-AldDH-NADHOx electrodes | 10 to 60 μ M | 2600 | [35] |
| Cyclic Voltammetry | Copper chloride modified copper electrode | 2 to 50mM | - | [36] |
| Amperometry | Aldehyde dehydrogenase and diaphorase on platinum electrode | 1 to 500 μ M | - | [37] |
| Cyclic Voltammetry | CeO ₂ -MWCNT/GC | 0.01 to 10 μ M | 7.4 | Present work |

Table 2: Analysis of synthetic fruit juice sample

| Components (g/100ml) | CH ₃ CHO spiked (M) | CH ₃ CHO found (M) | Recovery (%) |
|-------------------------|-----------------------------------|----------------------------------|-----------------|
| Glucose: 1 | 10 ⁻⁸ | 9.88x10 ⁻⁹ | 98.8 |
| Fructose: 1 | | | |
| Ethanol : 0.01 | 10 ⁻⁷ | 1.01x10 ⁻⁷ | 101.0 |
| Glycerol: 0.01 | | | |
| Potassium: 0.02 | | | |

Figure captions.

Fig.1 XRD pattern of CeO₂ and CeO₂-MWCNT nanocomposite

Fig.2 (a) SEM image of CeO₂ (b) MWCNT (c) CeO₂-MWCNT

Fig.3 UV-Visible absorption spectra of suspension of CeO₂ and CeO₂-MWCNT

Fig.4 Nyquist diagram of electrochemical impedance spectra of bare GC, CeO₂/GC and CeO₂-MWCNTs/GC electrodes in 0.1 M KNO₃ solution containing 5.0 mM Fe(CN)₆^{3-/4-} (1:1). The inset is equivalent circuit of CeO₂-MWCNT/GC electrochemical impedance measurement system

Fig.5 Cyclic voltammograms of bare GC, CeO₂/GC and CeO₂-MWCNT/GC electrodes in 1 mM K₃Fe(CN)₆ and 0.1 M KCl as supporting electrolyte at a scan rate of 50 mVs⁻¹

Fig.6 Cyclic voltammograms of acetaldehyde (10⁻⁶M) at bare GC, CeO₂/GC and CeO₂-MWCNT/GC modified electrodes in 0.1M KNO₃ as supporting electrolyte at a scan rate of 50 mVs⁻¹

Fig.7 (a) Cyclic voltammograms at the CeO₂-MWCNT/GC nanocomposite electrode in the presence of different concentrations of acetaldehyde (b) calibration curve in the range of 10⁻⁸ to 10⁻⁵ M of acetaldehyde (i) I_p vs. [acetaldehyde] (ii) I_p vs. log [acetaldehyde] plots

Fig. 8 Selectivity studies of acetaldehyde and other organics

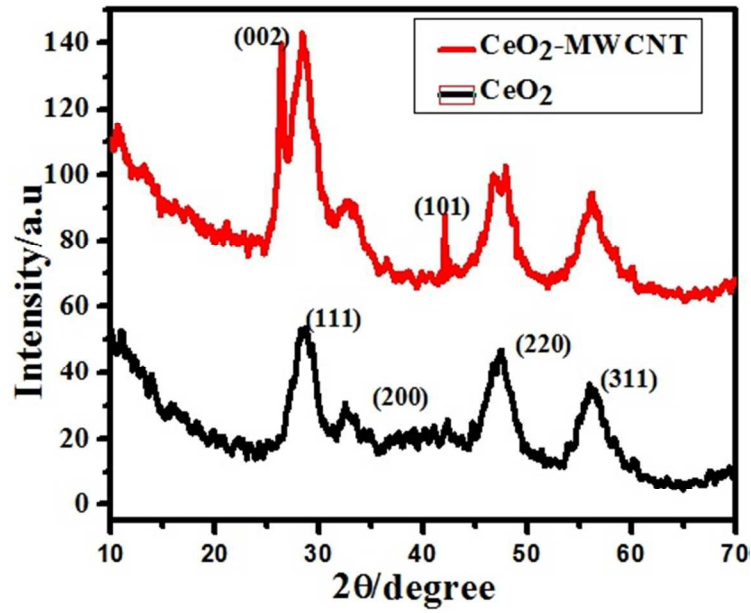


Fig. 1

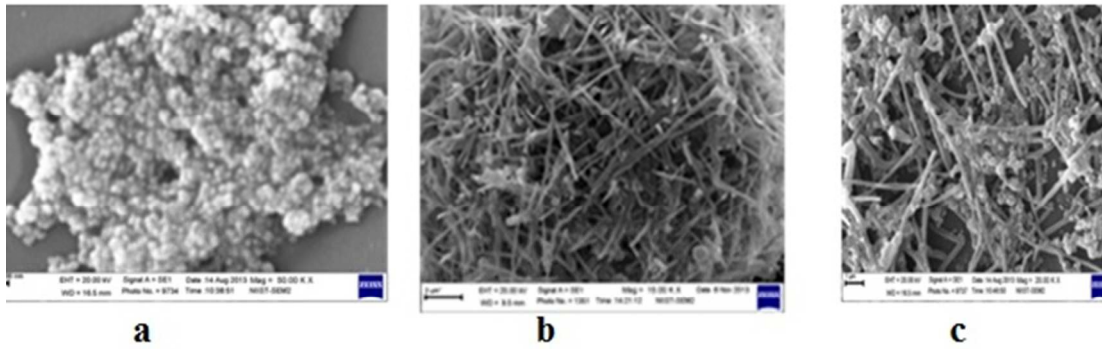


Fig. 2

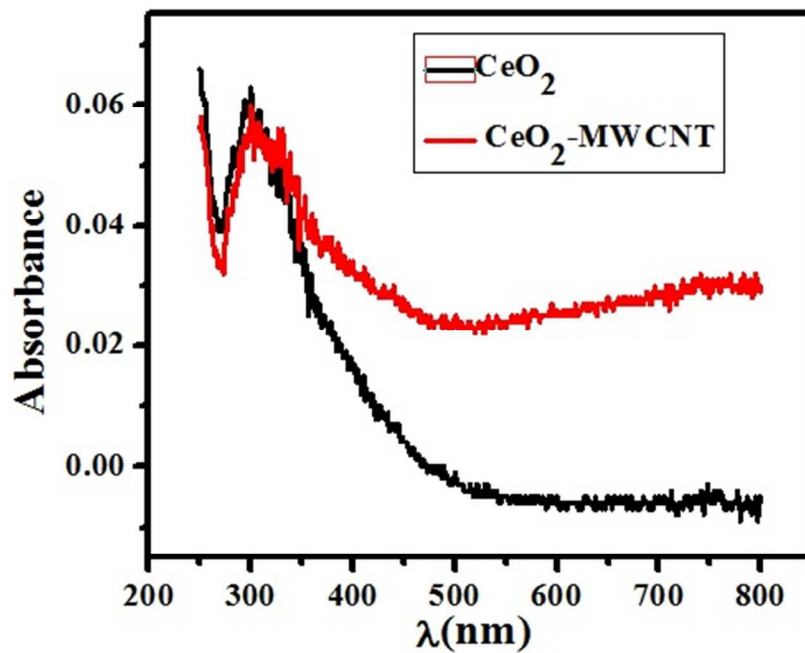


Fig. 3

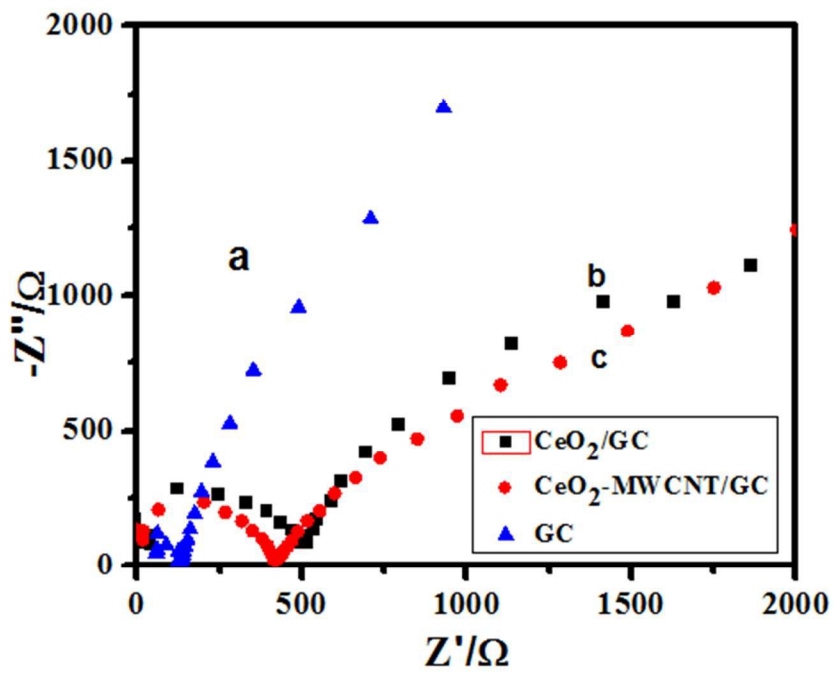


Fig. 4

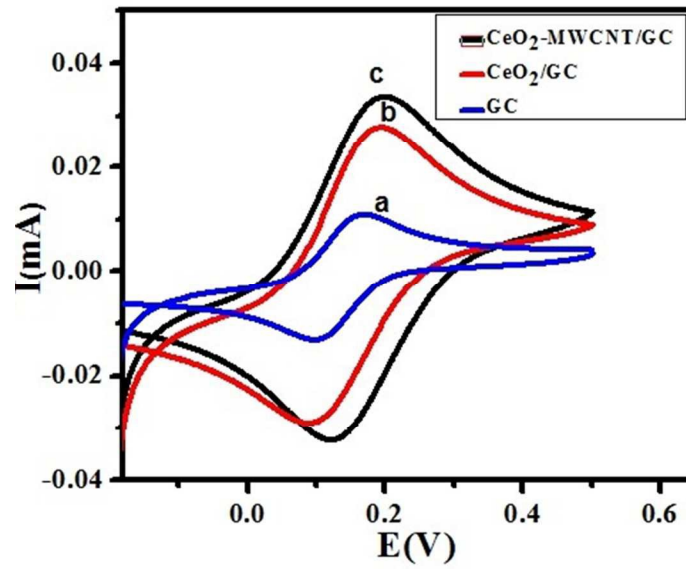


Fig. 5

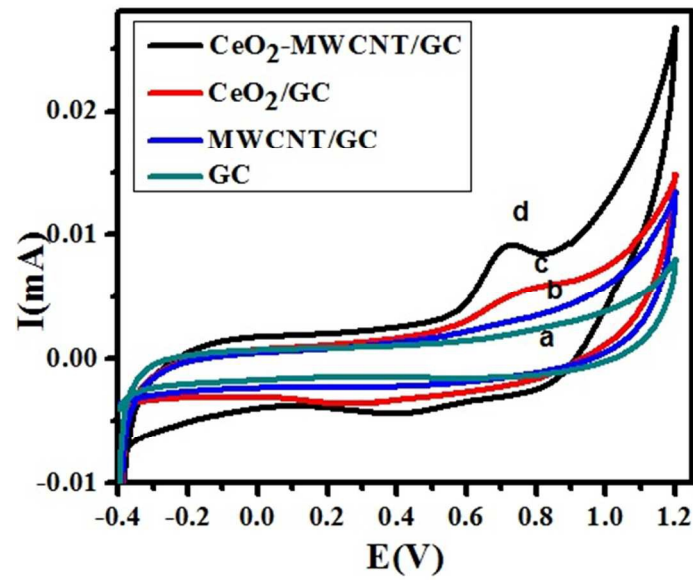


Fig. 6

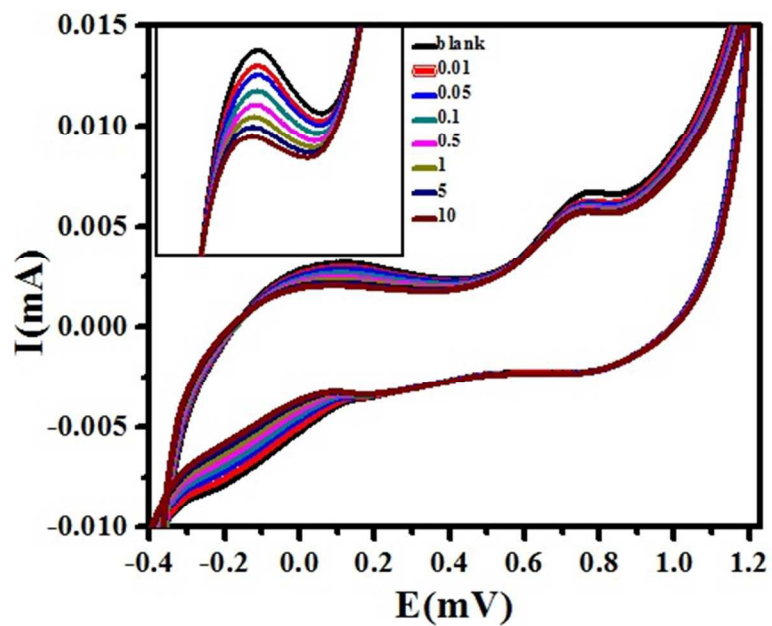


Fig. 7a

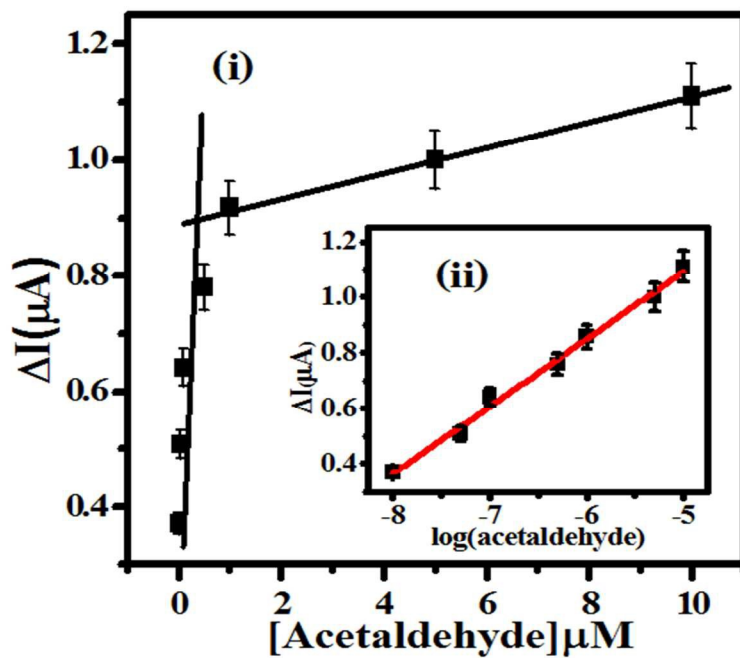


Fig. 7b

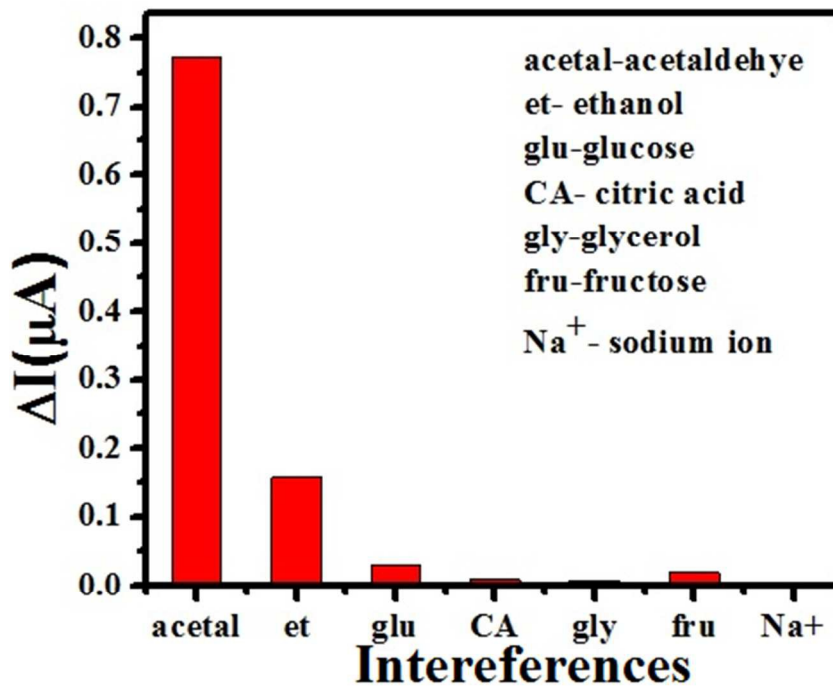
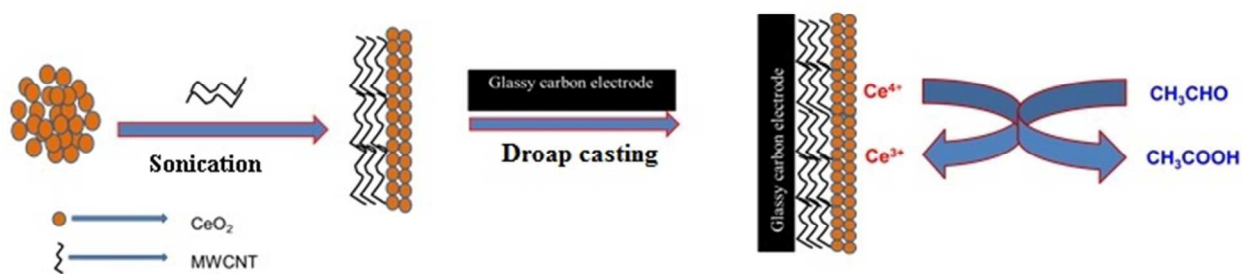


Fig. 8



Scheme 1